PROTEINS: Structure, Function, and Genetics 17:93–106 (1993)

Structural Analysis of the Zinc Hydroxide–Thr-199–Glu-106 Hydrogen-Bond Network in Human Carbonic Anhydrase II

Yafeng Xue,[1] Anders Liljas,[2] Bengt-Harald Jonsson,[1] and Sven Lindskog[1]
[1]Department of Biochemistry, University of Umeå, S-90187 Umeå, Sweden; and [2]Department of Molecular Biophysics, Chemical Center, University of Lund, S-22100 Lund, Sweden

ABSTRACT **The significance of the zinc hydroxide–Thr-199–Glu-106 hydrogen-bond network in the active site of human carbonic anhydrase II has been examined by X-ray crystallographic analyses of site-specific mutants. Mutants with Ala-199 and Ala-106 or Gln-106 have low catalytic activities, while a mutant with Asp-106 has almost full CO_2 hydration activity. The structures of these four mutants, as well as that of the bicarbonate complex of the mutant with Ala-199, have been determined at 1.7 to 2.2 Å resolution. Removal of the γ atoms of residue 199 leads to a distorted tetrahedral geometry at the zinc ion, and a catalytically important zinc-bound water molecule has moved towards Glu-106. In the bicarbonate complex of the mutant with Ala-199 one oxygen atom from bicarbonate binds to zinc without displacing this water molecule. Tetrahedral coordination geometries are retained in the mutants at position 106. The mutants with Ala-106 and Gln-106 have a zinc-bound sulfate ion, whereas this sulfate site is only partially occupied in the mutant with Asp-106. The hydrogen-bond network seems to be "reversed" in the mutants with Ala-106 and Gln-106. The network is preserved as in native enzyme in the mutant with Asp-106 but the side chain of Asp-106 is more extended than that of Glu-106 in the native enzyme. These results illustrate the importance of Glu-106 and Thr-199 for controlling the precise coordination geometry of the zinc ion and its ligand preferences which results in an optimal orientation of a zinc-bound hydroxide ion for an attack on the CO_2 substrate.**

Key words: catalytic mechanism, protein engineering, site-specific mutagenesis, substrate binding, X-ray crystallography

INTRODUCTION

Human carbonic anhydrase II (CAII, EC 4.2.1.1) is one of the most efficient of all known enzymes. It catalyzes the hydration of carbon dioxide to bicarbonate ion with a maximal turnover rate of about 10^6 s^{-1} at 25°C.[1] The enzyme contains one catalytically required zinc ion, which is coordinated to three histidine residues, His-94, His-96, and His-119. A tetrahedral coordination sphere is completed with a water molecule which forms a hydroxide ion with a pK_a value near 7. It is widely accepted that the central step of the reaction mechanism is a nucleophilic attack by the zinc-bound hydroxide ion on a carbon dioxide molecule located in a hydrophobic cavity in the vicinity.[1,2] The bicarbonate ion formed in this step is then displaced from the zinc ion by a water molecule. Regeneration of the zinc-bound hydroxide ion completes the catalytic cycle in a rate-determining proton-transfer process.[1]

The X-ray crystallographic analysis of human CAII has shown that the zinc-bound H_2O/OH^- is hydrogen bonded to the hydroxyl oxygen of Thr-199 which, in turn, is linked to one carboxylate oxygen of Glu-106. The other carboxylate oxygen of Glu-106 is hydrogen bonded to the amide NH of Arg-246 and also connected to the hydroxyl oxygen of Tyr-7 via a water molecule, thus completing a hydrogen-bond network extending from the zinc-bound H_2O/OH^- to Tyr-7.[3] Both Glu-106 and Thr-199 are conserved in all sequenced animal CA:s.[4] It has been proposed that these residues serve to orient a lone pair of the zinc-bound hydroxide ion properly for the attack on the carbon atom of the CO_2 molecule.[5] Furthermore, the binding of protonated anions to the metal ion seems to be favored due to the presence of these residues.[6–8] Recent crystallographic studies suggest that the network also prevents bicarbonate from binding with its negatively charged oxygen to the zinc ion[7,9] and, thus, obviates the need of proton transfer within bound bicarbonate before the formation of the transition state in the dehydration reaction.[10]

Abbreviations: CA, carbonic anhydrase; rms, root-mean-square; site-specific mutants are designated by the single-letter code for the original amino acid followed by the sequence number followed by the single-letter code for the new amino acid.

Received December 15, 1992; revision accepted April 7, 1993.

Address reprint requests to Dr. Sven Lindskog, Department of Biochemistry, University of Umeå, S-90187 Umeå, Sweden.

Results of kinetic studies of human CAII mutated at positions 106 and 199 confirmed that these two residues play critical roles in maintaining the high catalytic efficiency of the enzyme.[11] In this paper we examine the structural consequences of mutations of these active site residues using X-ray crystallography.

EXPERIMENTAL PROCEDURES

Proteins

The mutagenesis procedure has been described earlier.[11] The Thr-199 → Ala (T199A) mutant was purified by affinity chromatography according to the procedure of Khalifah et al.[12] with some modifications. Thus, 20 mM Tris/H_2SO_4 at pH 9.0 was used for binding and washing and 100 mM Tris/H_2SO_4 at pH 7.4 containing 400 mM NaN_3 was used for elution. An additional ion-exchange chromatography step (Y. Xue and B.-H. Jonsson, unpublished data)[13] was used to improve crystal quality. The mutants E106A, E106D, and E106Q, purified as described by Liang et al.,[11] were kindly provided by Z. Liang.

Crystallization

Crystals of all mutants were grown by the hanging drop method using 2.3 M $(NH_4)_2SO_4$ in 50 mM Tris/H_2SO_4 buffer, pH 8.5, containing 3 mM dithiothreitol which served to prevent formation of intermolecular disulfide bridges. The crystals appeared within 1 to 4 weeks at 4°C and typically showed a flattened plate shape with the smallest dimension of 0.05 mm. All the crystals belong to space group $P2_1$ and are isomorphous with native human CAII with unit cell parameters: a = 42.7 Å, b = 41.7 Å, c = 73.0 Å, and β = 104.6°.[3]

Data Collection

X-Ray intensity data were collected using a Siemens (Xentronics) multiwire area detector mounted on a Rigaku RU200HB rotating anode generator (CuK_α radiation opertating at 45 kV/90 mA, 0.3 × 3 mm focal spot, graphite monochromator). The detector was placed 8.5 cm from the crystal. The Siemens 3 axis goniostat with a fixed $\chi = 45°$ was used with 2θ ranging from 13° to 30° for different mutants. Two spindle (ϕ) angles (only one for E106Q and T199A) were used. The crystal was rotated 180° or more about ω, with a step size of 0.25° and an exposure time between 90 and 130 seconds per frame (Table I). All the data sets were collected from a single crystal. The reflection data were processed using the Xengen program suite[14] or the XDS package.[15,16] Data statistics are given in Table II and Table III.

Refinement

All calculations were done on a VAX workstation 3100. $2|F_o|-|F_c|$ and $|F_o|-|F_c|$ electron density maps were calculated with the CCP4 program package[17] and inspected at several stages on Evans & Sutherland PS390 and ESV graphics stations using the programs FRODO[18,19] and O.[20] The least squares refinement was carried out with the program PROFFT[21,22] refining both atomic positions and individual temperature factors. The starting model for the first electron density maps and the refinement was the refined structure of human CAII at 1.54 Å resolution[7] without the side chains of the mutated residues and the zinc-bound water molecule. Both $2|F_o|-|F_c|$ and $|F_o|-|F_c|$ maps were calculated and showed significant peaks at the locations of the mu-

TABLE I. Data Collection

Mutant	2θ (°)	Orientations	Exposure time (sec/frame)	Program for processing
T199A	13	1	90	Xengen
T199A/HCO_3^-	30	2	130	XDS
E106A	23	2	130	XDS
E106D	20	2	130	XDS
E106Q	20	1	120	Xengen

TABLE II. Statistics of Data Collection and Refinement for T199A-CAII

	T199A	T199A/HCO_3^-
Data collected		
No. of observations	22,118	53,784
No. of unique reflections	12,172	23,451
Completeness (%)	91.9	84.9
Max. resolution (Å)	2.2	1.7
R_{merge} (%)	7.9	4.0
Refinement		
No. of reflections used (1σ)	11,550	23,376*
Refinement R-value (%)	16.6	16.0
Error in coordinates (Å)	0.21	0.17
No. of protein atoms	2,057	2,057
No. of solvent atoms	209	214
rms values		
Bond distance (Å)	0.019	0.018
Angle distance (Å)	0.037	0.035
Planar 1–4 distance (Å)	0.045	0.045
Plane groups (Å)	0.017	0.018
Chiral centers (Å^3)	0.193	0.210
Single torsion (Å)	0.159	0.155
Multiple torsion (Å)	0.162	0.161
Possible X–Y H-bond (Å)	0.160	0.142
Torsion angles		
Planar (°)	3.2	3.5
Staggered (°)	18.2	15.8
Orthonormal (°)	30.1	30.1
Thermal restraints		
Main chain bond (Å^2)	0.925	0.942
Main chain angle (Å^2)	1.528	1.523
Side chain bond (Å^2)	1.732	2.089
Side chain angle (Å^2)	2.700	3.281

*All the data (0σ) used for refinement.

TABLE III. Statistics of Data Collection and Refinement for E106A, E106D, and E106Q

	E106A	E106D	E106Q
Data collected			
No. of observations	34,070	33,101	26,134
No. of unique reflections	20,430	17,315	14,073
Completeness (%)	87.6	87.0	72.2
Max. resolution (Å)	1.8	1.9	1.9
R_{merge} (%)	6.2	5.6	7.3
Refinement			
No. of reflections used (1σ)	18,689	16,149	13,911*
Refinement R-value (%)	16.1	15.1	16.0
Error in coordinates (Å)	0.17	0.16	0.18
No. of protein atoms	2,055	2,058	2,059
No. of solvent atoms	206	208	209
rms values			
Bond distance (Å)	0.021	0.020	0.022
Angle distance (Å)	0.040	0.038	0.039
Planar 1–4 distance (Å)	0.049	0.048	0.051
Plane groups (Å)	0.018	0.018	0.019
Chiral centers (Å^3)	0.200	0.196	0.207
Single torsion (Å)	0.161	0.158	0.161
Multiple torsion (Å)	0.162	0.162	0.168
Possible X–Y H-bond (Å)	0.166	0.166	0.162
Torsion angles			
Planar (°)	3.4	3.4	3.4
Staggered (°)	16.4	16.5	17.8
Orthonormal (°)	30.7	32.2	31.1
Thermal restraints			
Main chain bond (Å^2)	1.034	0.978	1.039
Main chain angle (Å^2)	1.655	1.609	1.632
Side chain bond (Å^2)	2.086	2.075	2.015
Side chain angle (Å^2)	3.217	3.237	3.125

*All the data (0σ) used for refinement.

tated residues. The mutated residues were then built into the model. Manual adjustments were made after inspection of the maps, and solvents molecules with B factors larger than 65 were removed from the model before the next round of refinement. The ring atoms of imidazoles were identified solely by their hydrogen bond neighbors.

The final R-factors were between 15.1 and 16.6% for the five structures with root-mean square (rms) deviations from ideal bond lengths and angle-related distances within the ranges 0.018–0.022 and 0.035–0.040 Å, respectively. Pertinent refinement statistics are given in Tables II and III. Overall mean errors in the atomic coordinates were estimated to be within the range 0.16–0.21 Å by the method of Luzzati.[23]

Identification of Extraneous Zinc Ligands

After a few cycles of refinement of the mutant model, a well-shaped tetrahedral density appeared at the zinc ion in both $2|F_o|-|F_c|$ and $|F_o|-|F_c|$ maps for mutants at position 106 (Figs. 1–3). The central part of the difference density reached a level of >20 σ for E106A and E106Q. Considering the composition of the crystallization medium, this density was interpreted as a sulfate ion and built into the model. This interpretation was supported by the results of kinetic studies of the inhibition by sulfate of CO_2 hydration catalyzed by these mutants.[11] The peak level of the density is about 13 σ for the mutant E106D, and a negative density appeared in the difference map after inserting the sulfate ion. Therefore, this ligand density was interpreted as composed partially of a sulfate ion and partially of a water molecule, and this resulted in a well defined density after refinement (Fig. 3).

In the case of the mutant T199A, two data sets (1.8 Å and 2.2 Å resolution, respectively) were collected at an early stage of the work. Significant densities, apparently corresponding to two non-protein ligands, were observed at the zinc ion in the $2|F_o|-|F_c|$ and the $|F_o|-|F_c|$ maps after a few cycles of refinement of the mutant model. For the 2.2 Å data set, two spherically shaped densities were observed at the zinc ion (Fig. 4). For the 1.8 Å data set (data not shown), one of the densities is larger and flattened. The highest level of this difference density was about 14σ. Considering that atmospheric carbon dioxide might have been absorbed in the alkaline crystallization medium (pH 8.5) and the shape

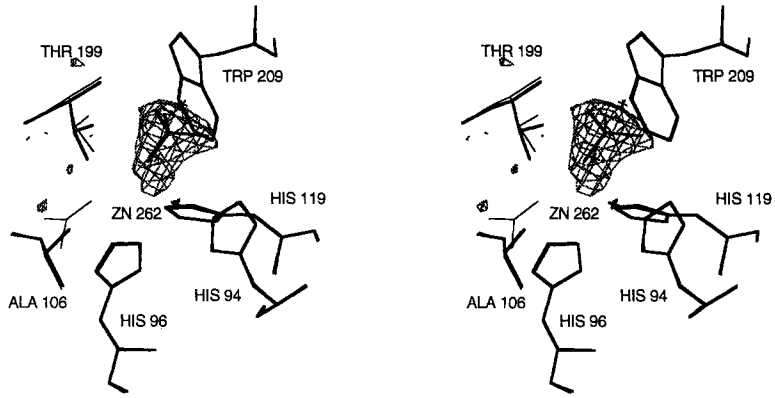

Fig. 1. Stereo view of the $|F_o|-|F_c|$ difference map showing the bound sulfate ion in E106A-CAII. The phase angles were obtained from the refined coordinates of the unmodified enzyme[7] where Wat263, Wat318, and Wat338 were deleted before calculating the map. The positions of Wat263 and Wat338 in the unmodified enzyme are indicated by thin crosses. Thin lines represent the unmodified enzyme. Contours are drawn at $+5\sigma$.

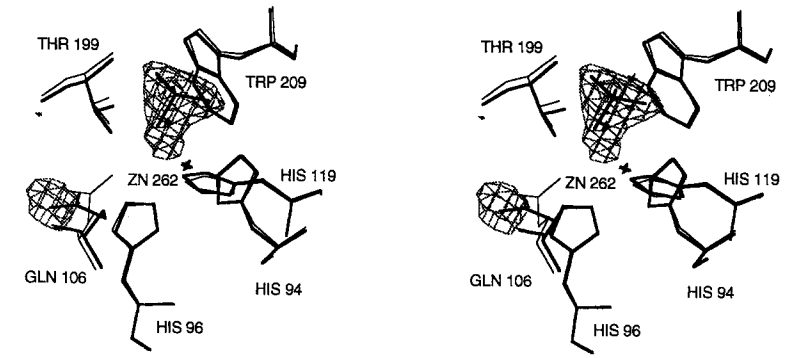

Fig. 2. Stereo view of the $|F_o|-|F_c|$ difference map showing the bound sulfate ion in E106Q-CAII. The phase angles were obtained from the refined coordinates of the unmodified enzyme[7] where Wat263, Wat318, and Wat338 were deleted before calculating the map. The positions of Wat263 and Wat338 in the unmodified enzyme are shown by thin crosses. Thin lines represent the unmodified enzyme. The density at the side chain of residue 106 results from the mutation. Contours are drawn at $+5\sigma$.

of the density (a triangular and near-planar shape with moderate peak height), the peak was tentatively interpreted as originating from a bicarbonate ion. Tris and sulfate were also considered but did not fit the density. No other ions had been added to the solution. This interpretation was supported by subsequent data on the binding of bicarbonate to T199A (K_d = 15 mM at pH 8.5 and 4 mM at pH 7.5[11]). However, a strained geometry between these two new ligands was observed in the refined model presumably arising from local disorder or other species than bicarbonate also present at the same position. Presumably, the concentration of HCO_3^- in the mother liquor was too low to saturate the binding site in spite of the relatively high affinity. The results presented below on the structure of T199A-CAII were obtained from the 2.2 Å data set, but since no special precautions were taken to avoid contamination by carbon dioxide, it cannot be excluded that these data also are affected by contributions from bound HCO_3^-.

To establish the identity of this putative HCO_3^- ligand, a new data set was collected to 1.7 Å resolution after soaking the T199A crystal in a solution containing 0.8 M ammonium bicarbonate, 2.4 M ammonium sulfate and 50 mM Tris-sulfate buffer, pH 7.6, for 18 hours. In both the $2|F_o|-|F_c|$ and $|F_o|-|F_c|$ maps calculated from the mutant model, a well defined triangular, near-planar density was evident in accordance with the presence of a bicarbonate ion (Fig. 5).

RESULTS

The Structure of T199A-CAII

The overall structure of the mutant is very similar to that of native human CAII. The rms difference in atomic coordinates compared to the structure of the native enzyme is 0.25 Å, while the corresponding difference for the Cα atoms is 0.12 Å and the shift of Cα of residue 199 is 0.15 Å. The most significant movement of protein atoms is a shift of the side chain of Leu-198 (rms deviation, 0.5 Å). The ε atoms

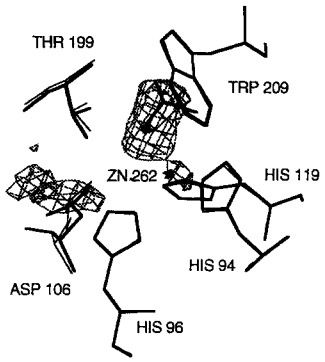

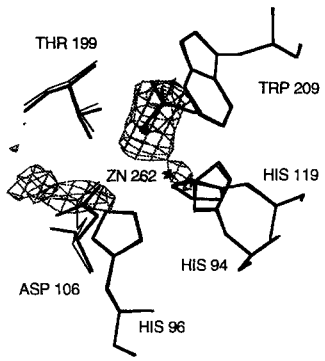

Fig. 3. Stereo view of the $|F_o|-|F_c|$ difference map showing the density of non-protein ligands at zinc in E106D-CAII. The phase angles were obtained from the refined coordinates of the unmodified enzyme[7] where Wat263, Wat318, and Wat338 were deleted before calculating the map. A sulfate ion and a water molecule are both bound to the metal ion with partial occupancies. The position of the water molecule is indicated by a heavy cross within the density, while the position of Wat338 in the unmodified enzyme is indicated by a thin cross. The structure of the unmodified enzyme is shown by thin lines. The density near the side chain of residue 106 results from the mutation. Contours are drawn at $+4\sigma$.

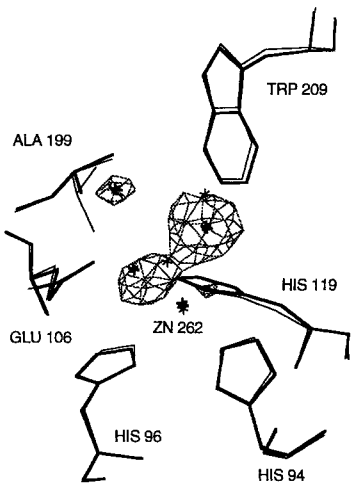

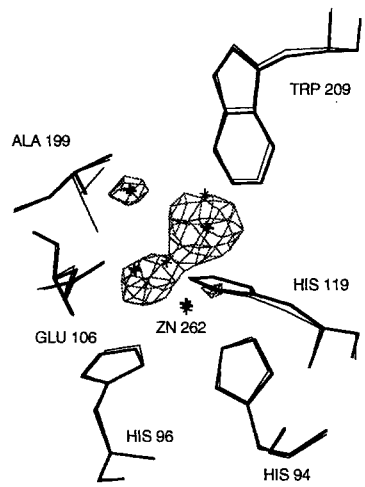

Fig. 4. Stereo view of the $|F_o|-|F_c|$ difference map showing the two solvent molecules (Wat263 and Wat338) close to the metal in T199A-CAII. The phase angles were obtained from the refined coordinates of the unmodified enzyme[7] where Wat263 and Wat338 were deleted before calculating the map. The positions of these water molecules in the native enzyme are indicated by thin crosses, while the crosses drawn enhanced correspond to their positions as well as the position of Wat501 in the mutant. Thin lines refer to the structure of unmodified enzyme. Contours are drawn at $+5\sigma$.

of Glu-106 remain in the same position as in the native enzyme but appear to be more mobile with a temperature factor of 13.6 Å^2 compared to 7.3 Å^2 in the native enzyme. Considering an error in the atomic coordinates of about 0.2 Å, the removal of the γ atoms of residue 199 has resulted in almost insignificant perturbations of the rest of the protein structure.

Two solvent molecules in the close vicinity of zinc, Wat263 and Wat338 (Fig. 4), were refined. Their temperature factors are 12.6 and 11.3 Å^2, respectively. The corresponding water molecules in native CAII are referred to as the zinc-bound water and the "deep" water, respectively.[3,7] A significant density was clearly seen for Wat338, whereas a poorly shaped density was observed for Wat263 in the $2|F_o|-|F_c|$ map calculated from the refined model.

The coordination geometry of the zinc ion can be described as distorted tetrahedral (Table IVB). The zinc-bound H_2O/OH^- (Wat263) has moved 1.2 Å to a new position which is 2.2 Å from zinc, 3.2 Å from Cβ of Ala-199 (4.0 Å from Cβ of Thr-199 in the native enzyme), 3.2 Å from Oϵ1 of Glu-106 (4.3 Å in the native enzyme), and 2.0 Å from the position of Oγ1 of Thr-199 in the native enzyme (Fig. 6). Thus, it appears that the zinc-bound H_2O/OH^- has moved into a more buried position as a consequence of the removal of the side chain of residue 199. Wat338, the electron density of which might be perturbed by the presence of some bound HCO_3^-, seems to have moved 1.1 Å to a position only 2.9 Å from the zinc ion. Wat338 is hydrogen bonded to Wat263 (O–O distance, 2.8 Å) as in native CAII but is 4.0 Å from the amide nitrogen of residue 199, which has no con-

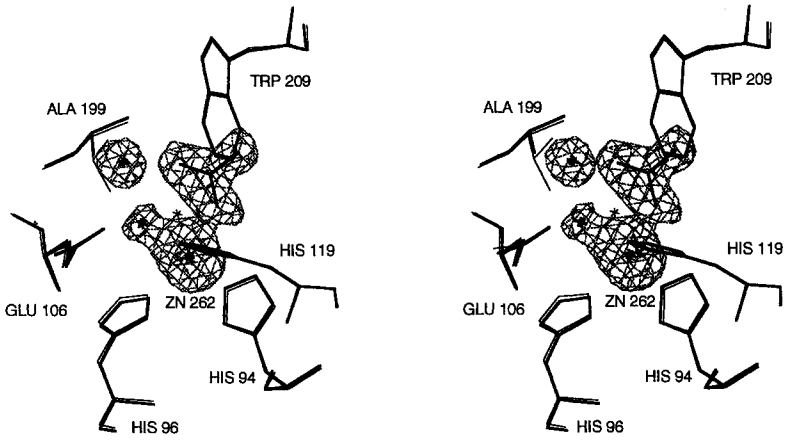

Fig. 5. Stereo view of the $|F_o|-|F_c|$ difference map showing the zinc-bound bicarbonate ion and water molecule in the T199A/HCO_3^- complex. The phase angles were obtained from the refined coordinates of the unmodified enzyme[7] where zinc, Wat263, and Wat338 were deleted before calculating the map. The thin cross between the densities indicates the zinc-water position in unmodified CAII, while thick crosses show the positions of zinc, Wat263 and Wat501 in the mutant. Thin lines show the structure of the unmodified enzyme. Contours are drawn at $+4\sigma$.

TABLE IVA. Geometry of the Zinc Ion in Wild-Type Human CAII*

		Angle (°)		
	Distance (Å)	X-Zn-94	X-Zn-96	X-Zn-119
OH-263	2.1	111.1	113.6	112.9
Nε2 94	2.1		103.9	115.3
Nε2 96	2.1			99.2
Nδ1 119	2.1			

*Coordinates from Håkansson et al.[7]

TABLE IVB. Geometry of the Zinc Ion in T199A-CAII

		Angle (°)			
	Distance (Å)	X-Zn-94	X-Zn-96	X-Zn-119	X-Zn-(O-338)
OH-263	2.2	122.2	81.2	121.0	65.9
Nε2 94	2.4		96.5	115.0	102.9
Nε2 96	2.3			106.6	147.0
Nδ1 119	2.2				89.2
O-338	2.9				

tacts within 3.3 Å. Another water molecule, Wat318, linking the zinc-bound H_2O/OH^- and the rest of the water structure in the native enzyme,[9] has shifted 1.4 Å and is close to Wat338 (O–O distance, 2.6 Å).

The mutation has resulted in additional, significant perturbations of the solvent structure in the active site (data not shown). Interestingly, a new water molecule, Wat501 with a temperature factor of 15.1 Å^2, was found 3.3 Å from Cβ of Ala-199, apparently to fill up the space created by the mutation (Figs. 4 and 6). This water molecule is hydrogen bonded to Oε1 of Glu-106 (O–O distance, 2.8 Å) and is 3.4 Å from Cε1 of His-107 and 5.5 Å from zinc.

A single orientation of His-64 was observed. It corresponds to the major conformation found in the crystal structure of native CAII[7,9] except that the imidazole ring has rotated 180° as judged from the putative hydrogen-bond contacts.

The Structure of the Bicarbonate Complex of T199A-CAII

The rms difference in atomic coordinates compared to those of the native enzyme is 0.15 Å, while Cα of residue 199 has shifted 0.18 Å. In the refined model, the zinc-bound water molecule and the bicarbonate ion have temperature factors of 9.8 and 13.8 Å^2, respectively, indicating that bicarbonate is bound to the enzyme with nearly full occupancy.

A penta-coordination of the zinc ion was observed (Figs. 5 and 7). Thus, a water molecule (Wat263) is located 2.2 Å from the zinc ion, 1.6 Å from the position of the zinc-bound H_2O/OH^- in the native en-

TABLE IVC. Geometry of the Zinc Ion in the T199A/HCO_3^- Complex

		Angle (°)			
	Distance (Å)	X-Zn-94	X-Zn-96	X-ZN-119	X-Zn-O3(HCO_3^-)
OH-263	2.2	136.6	81.4	110.7	82.7
Nε2 94	2.1		95.0	112.7	88.1
Nε2 96	2.2			97.6	159.9
Nδ1 119	2.1				99.5
O3(HCO_3^-)	2.3				

TABLE IVD. Geometry of the Zinc Ion in E106A-CAII

		Angle (°)			
	Distance (Å)	X-Zn-94	X-Zn-96	X-Zn-119	X-Zn-O4 (SO_4^{2-})
O2(SO_4)	2.1	112.2	103.2	116.0	55.1
Nε2 94	2.2		103.8	116.2	77.9
Nε2 96	2.1			103.2	155.4
Nδ1 119	2.1				97.8
O4(SO_4^{2-})	3.0				

TABLE IVE. Geometry of the Zinc Ion in E106Q-CAII

		Angle (°)			
	Distance (Å)	X-Zn-94	X-Zn-96	X-Zn-119	X-Zn-O4(SO_4^{2-})
O2(SO_4)	2.1	112.9	100.4	117.9	55.6
Nε2 94	2.2		102.9	117.0	81.2
Nε2 96	2.2			102.0	154.1
Nδ1 119	2.2				98.5
O4(SO_4^{2-})	2.9				

TABLE IVF. Geometry of the Zinc Ion in E106D-CAII

		Angle (°)			
	Distance (Å)	X-Zn-94	X-Zn-96	X-Zn-119	X-Zn-O4(SO_4^{2-})
OH-263*	2.2	106.5	112.4	114.1	52.1
O2(SO_4)*	2.2	112.7	107.9	111.4	56.9
Nε2 94	2.2		106.4	117.4	79.1
Nε2 96	2.2			99.8	164.4
Nδ1 119	2.1				90.2
O4(SO_4^{2-})	2.9				

*Binding at the same site with partial occupancy.

zyme and 1.7 Å from the position of Oγ1 of Thr-199 in the native enzyme. In addition, one bicarbonate oxygen (O3) is coordinated to the zinc ion at a distance of 2.3 Å and 4.1 Å from the position of Oγ1 of Thr-199 in the native enzyme. The coordination geometry is close to that of a trigonal bipyramid with bicarbonate and His-96 at the two axial positions (Table IVC). The liganded bicarbonate oxygen is located 1.5 Å from the position of the zinc-bound H_2O/OH^- in the native enzyme. Another bicarbonate oxygen is hydrogen bonded both to the amide NH of Ala-199 (O–N distance, 2.7 Å) and to the coordinated water molecule (O–O distance, 2.7 Å). The third oxygen is located 4.4 Å from the zinc ion and points into the hydrophobic region. It is hydrogen bonded to a water molecule, Wat389, located 5.3 Å from the zinc ion (O–O distance, 2.6 Å). In comparison with the structure of uncomplexed T199A-CAII, the zinc-bound water molecule has moved 0.5 Å towards Oε1 of Glu-106 (O–O distance, 2.7 Å). Wat501 is still present in the bicarbonate complex and hydrogen bonded to Oε1 of Glu-106 (O–O distance, 3.0 Å).

As indicated in Figures 7 and 8, two of the bicarbonate oxygen atoms have similar positions (shifts of 0.4 Å and 0.5 Å) in the complexes with T199A-CAII and T200H-CAII.[9] The two binding modes are related by a 166° rotation of the bicarbonate ion

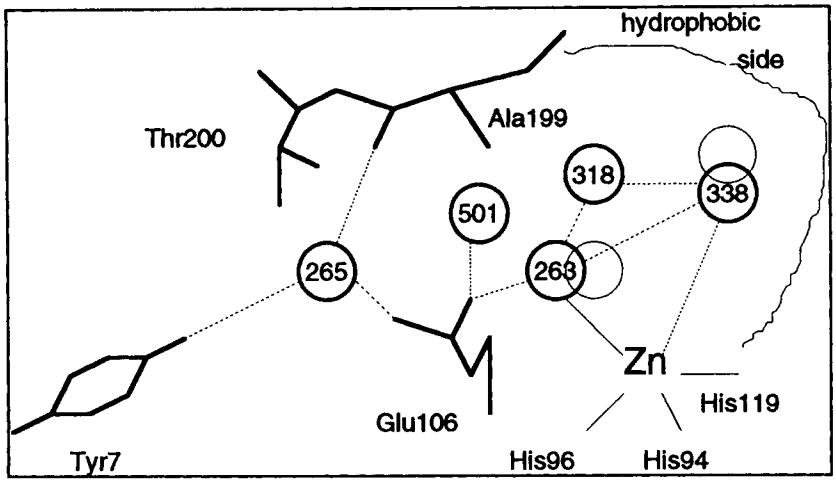

Fig. 6. Schematic diagram of the active site of T199A-CAII. The circles in thin lines indicate positions of water molecules in native CAII. Hydrogen bonds are indicated by dashed lines. The relatively short distance between zinc and Wat338 is also indicated by a dashed line. A new water molecule, Wat501, not present in the native enzyme, was found close to the position of the removed γ atoms of residue 199.

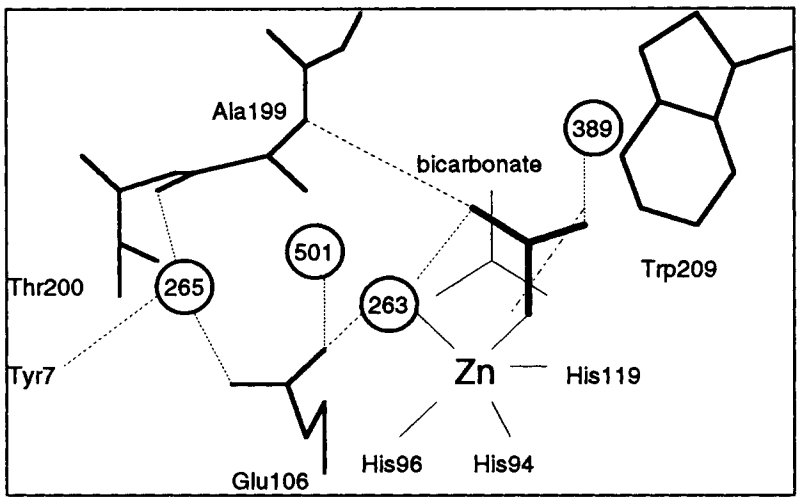

Fig. 7. Schematic diagram of bicarbonate bound to T199A-CAII. The position of bicarbonate bound to T200H-CAII[9] is shown by thin lines. The position of SCN^- bound to native CAII[6] is shown by the dot-dashed line. Hydrogen bonds are indicated by dashed lines.

about the axis defined by these oxygen atoms. This rotation involves the movement of the oxygen atom which is coordinated to the zinc ion and hydrogen bonded to Thr-199 in T200H-CAII to a position in T199A-CAII which is 4.0 Å from Cδ2 of Leu-198 in the hydrophobic cavity. It is also interesting to note that the binding mode of bicarbonate in T199A-CAII is similar to that of SCN^- in the native enzyme.[6] Two bicarbonate oxygen atoms are located within 0.4 Å of the positions of the two non-carbon atoms of SCN^- (Fig. 7).

Two orientations of His-64 corresponding to those observed in the native enzyme were refined to about equal proportion. The electron density for the side chain of His-64 is poorly shaped indicating a high mobility of the imidazole ring.

The Structure of E106A-CAII

The rms difference in atomic coordinates compared to those of the native enzyme is 0.20 Å, the Cα of residue 106 has moved 0.3 Å and the Cαs from residue 198 to residue 204 have moved between 0.2 and 0.5 Å. The side chain atoms of Thr-199 and Thr-200 have moved 0.5 and 0.7 Å, respectively. A metal-bound sulfate ion shows a well defined density in the refined model with a temperature factor of 16.0 Å^2 (Fig. 1).

The tetrahedral geometry of the zinc ion is maintained (Table IVD). The zinc-bound H_2O/OH^- present in native CAII is replaced by one sulfate oxygen with a difference in position of 0.5 Å (Zn-O distance, 2.1 Å). The hydrogen-bond between the liganded oxygen and Oγ1 of Thr-199 has been pre-

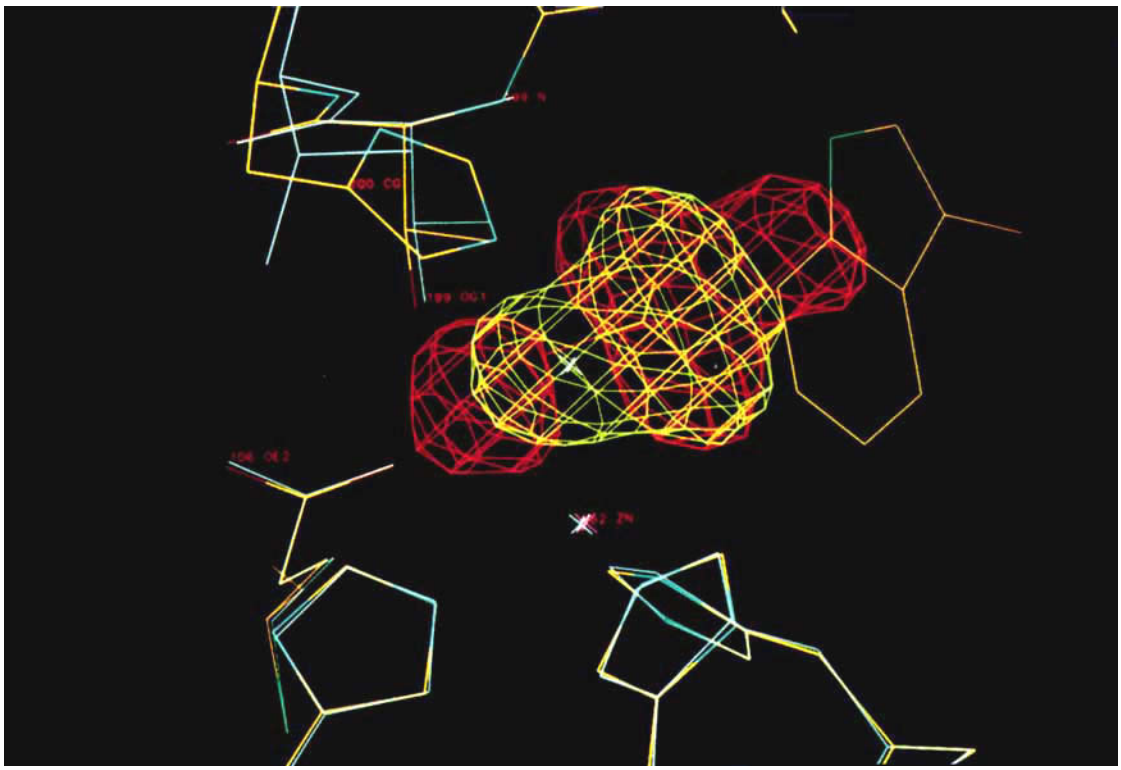

Fig. 8. Superposition of the $|F_o|-|F_c|$ difference maps showing bicarbonate bound to T200H-CAII (yellow) and bicarbonate (and the zinc-bound water molecule) bound to T199A-CAII (red). Lines in white show the structure in native CAII. Contours are drawn at $+4\sigma$.

served (O–O distance 2.9 Å). The sulfur atom is 2.9 Å from the zinc ion. The other three oxygen atoms of the sulfate ion have different hydrogen bond contacts. One of these oxygen atoms is situated near the hydrophobic region of the active site cavity 3.9 Å from Cγ2 of Val-121 and 4.2 Å from Cδ2 of Leu-198. This atom is 3.0 Å from the zinc ion and 3.1 Å from a water molecule, Wat359 (Fig. 9). Another oxygen atom is hydrogen bonded to the amide nitrogen of Thr-199 (O–N distance, 2.9 Å). It is located 0.9 Å from the position of the "deep" water molecule (Wat338), which it has displaced, and 3.5 Å from Cζ2 of Trp-209. The third oxygen is pointing towards the active-site entrance at a distance of 7.1 Å from Nε2 of His-64. This oxygen atom might form a hydrogen bond with Oγ of Thr-200 (the O–O distance is 3.3 Å and the geometry is reasonable).

This binding mode of sulfate resembles the binding of bicarbonate in T200H (Fig. 9), with three of the sulfate oxygen atoms shifted between 0.4 and 0.6 Å relative to the positions of the three bicarbonate oxygen atoms in T200H.[9]

A new water molecule, Wat501 (B factor, 18.7 Å^2), was observed in the position of the removed side chain of residue 106 (O–Cβ distance, 3.8 Å). It is hydrogen-bonded both to Oγ1 of Thr-199 and to Wat265 (Fig. 9), which is linked to Tyr-7 (O–O distances, 2.6 and 2.4 Å, respectively), and is located 3.2 Å from the amide NH of Arg-246, which is hydrogen bonded to a carboxylate oxygen of Glu-106 in the native structure. The temperature factor of Wat265 is 28.7 Å^2 whereas it is 8.1 Å^2 in native human CAII. Thr-199 is more mobile than in the native enzyme as indicated by an increase of the temperature factor from 5.2 Å^2 in native CAII to 11.9 Å^2 in the mutant. In addition, the hydrogen-bond pattern must have been "reversed" so that the hydroxyl group of Thr-199 now acts as a donor in the hydrogen bond with the zinc-bound oxygen atom from sulfate and, therefore, acts as an acceptor in the hydrogen bond with Wat501.

Two orientations were refined for the imidazole side chain of His-64, but the ring carbons and nitrogens cannot be conclusively defined by their hydrogen bond contacts.

The network of ordered water molecules is reorganized in the active site. Five water molecules have been displaced including the zinc-bound water (Wat263), the deep water (Wat338), and the water molecule (Wat318) connecting the zinc-bound water to the rest of the water network.

The Structure of E106Q-CAII

The rms difference in atomic coordinates compared to those of native CAII is 0.25 Å, while Cα of residue 106 has moved 0.3 Å. A sulfate ion bound to

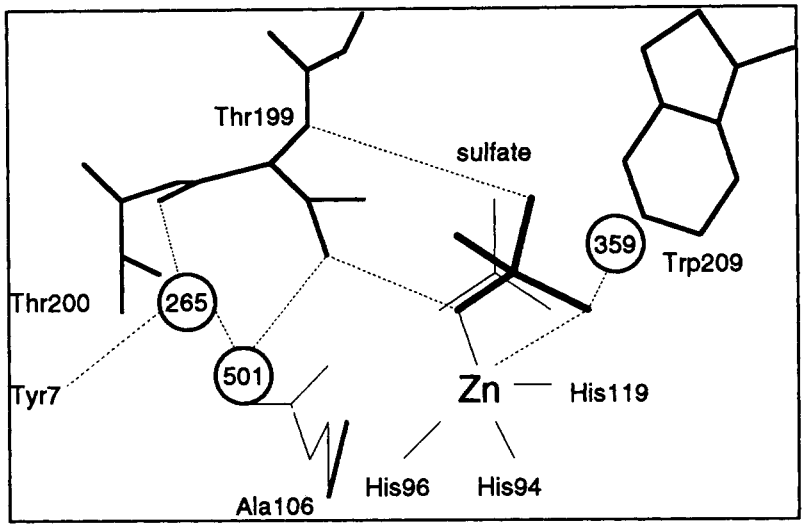

Fig. 9. Schematic diagram of the active site of E106A-CAII with a bound sulfate ion. The positions of bicarbonate in the complex with T200H-CAII[9] and the side chain of Glu-106 in native CAII are shown by thin lines. A new water molecule, Wat501, is hydrogen bonded to Wat265 and to Oγ1 of Thr-199.

the zinc ion was refined to a high occupancy with a temperature factor of 17.1 Å^2 (Fig. 2). Its location is very similar to that in E106A and the positions of the sulfur atoms differ by less than 0.3 Å. The tetrahedral geometry of the zinc ion is maintained (Table IVE) and is virtually identical to that found for E106A (Table IVD). The hydrogen-bond distance between the liganded oxygen and Oγ1 of Thr-199 is now 2.8 Å. The sulfur atom is 3.0 Å from the zinc ion and has moved 0.3 Å towards the active-site entrance relative its position in E106A-CAII.

Gln-106 is more exposed to solvent than Glu-106 in the native enzyme. Its Cα is shifted by 0.3 Å and the side chain has undergone significant rotations, about 70° around the Cβ–Cγ bond axis and 100° around the Cγ–Cδ bond axis. The ϵ atoms of residue 106 have moved away from the zinc ion and the Nϵ–Zn distance is 5.1 Å compared to an Oϵ–Zn distance of 4.1 Å in the native structure (Figs. 2 and 10). The identification of the two ϵ atoms of Gln-106 was solely based on the donor–acceptor requirements of hydrogen-bonded pairs of atoms. One ϵ atom was assigned as Oϵ, since it remains hydrogen bonded to the amide NH of Arg-246. Thus, the other ϵ atom was identified as Nϵ. The hydrogen-bond network in the active site is retained with Oϵ of Glu-106 replaced by Nϵ of Gln-106. The Nϵ atom of Gln-106 is hydrogen bonded both to Oγ1 of Thr-199 and to Wat265 (N–O distances, 2.9 Å in both cases). In the structure of native CAII, Oγ1 of Thr-199 and Wat265 are hydrogen bonded to one each of the two Oϵ atoms of Glu-106.[7,9] Since Nϵ of Gln-106 must act as a hydrogen-bond donor in the interaction with Thr-199, and Thr-199 must be a donor in its hydrogen bond with the metal-coordinated sulfate ion, a similarly "reversed" hydrogen-bond network is present in the mutant with Gln-106 as in the mutant with Ala-106.

In addition to the rotation of the side chain of residue 106, significant shifts were observed for atoms from residues 199 to 203 (Cα shifts of about 0.4 Å) and from residues 245 to 248 (Cα shifts of 0.3–0.9 Å). Such movements probably reflect compensatory effects due to the mutation. Thus, the main chain atoms from residues 245 to 248 (forming part of the active-site "wall") have moved away from the active site cavity in the same direction as the side chain of residue 106. The amide N(246)–Zn distance is 0.6 Å longer than in the native enzyme. The shifts of atoms from residues 199 to 203 along the wall of the active site towards the side chain of residue 106 compensate for the increase in space caused by the movement of this residue.

Only one orientation of the imidazole ring of His-64, similar to that found in the uncomplexed T199A mutant, was observed. The hydrogen bond distance between Nδ1 of His-64 and Wat332 is 2.6 Å, Another ring atom, Cδ2, is 3.1 Å from Wat292, also with a reasonable hydrogen-bond geometry, indicating that the imidazole ring is flipping. The hydrogen-bond contacts of the imidazole ring nitrogen atoms are different from those in the native enzyme.[7,9]

The network of ordered water molecules is reorganized in the active site and is similar to that found for E106A. Wat381, displaced in the structure of E016A-CAII, is present in E106Q-CAII (B factor, 42.5 Å^2).

A spherical density near Sγ of Cys-206 was observed. This density is not directly associated with the sulfur atom although its location is very similar to the mercury binding site found for crystals grown in the presence of methylmercury or mercuric

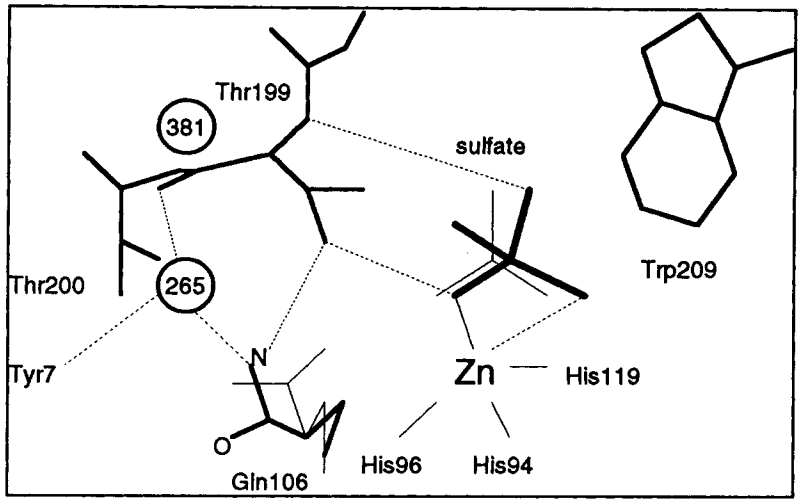

Fig. 10. Schematic diagram of the active site of E106Q-CAII with a bound sulfate ion. The positions of bicarbonate in the complex with T200H-CAII and the side chain of Glu-106 in native CAII are shown by thin lines.

ions.[2,6] This density probably arises from some impurity, perhaps a metal ion, in the crystallization medium. A metal atom was built into this density during refinement but its chemical identity remains unknown. Noting that this site is very close to the surface of the protein and 16 Å from the active site, a final identification of this density will not affect the overall structure or the most interesting part of the structure.

The Structure of E106D-CAII

Compared with the structure of native human CAII, the rms deviation of all atoms is 0.19 Å and Cα of residue 106 has moved 0.4 Å. Looking into the active site cavity from the entrance, the hydrophilic side has widened somewhat, apparently because of the shorter side chain of Asp-106 (Fig. 3). The zinc-bound H_2O/OH^- is 3.0 Å from Oγ1 of Thr-199 (2.8 Å in native CAII) and 4.6 Å from Oδ1 of Asp-106 (corresponding distance is 4.3 Å in native CAII). The shortest distance between the zinc ion and a carboxyl oxygen of residue 106 is 4.3 Å compared to 4.1 Å in the native enzyme. Although the overall pattern of the hydrogen bond network has been maintained, its geometry relative to zinc has shifted slightly (Fig. 11).

The hydrogen bond between the carboxyl oxygen (Oδ1) of residue 106 and Oγ1 of Thr-199 is preserved (O–O distance, 2.6 Å). The other δ oxygen atom of Asp-106 is still hydrogen bonded to the amide NH of Arg-246 (O–N distance is 3.0 Å compared to 2.9 Å in native CAII). Wat265, which has moved 0.9 Å from its position in native CAII (Fig. 11), appears to have weaker hydrogen bond contacts than in the native enzyme. It is 2.9 Å (2.6 Å in native CAII) from OH of Tyr-7, 3.1 Å (2.9 Å in native CA II) from the carbonyl O of Thr-199, and it is 3.2 Å from Oγ1 of Thr-199 and from Oδ2 of Asp-106. The distance between Wat265 and Oγ1 of Thr-199 is 3.6 Å in native CAII. Three water molecules, including the deep water, Wat338, have been displaced.

The putative sulfate ion was refined to about half occupancy (Fig. 3). The zinc-bound H_2O/OH^- (partial occupancy) is very close to its position in native CAII and also close to the position of the zinc-bound sulfate oxygen. It is 3.0 Å from Oγ1 of Thr-199 (Fig. 11). Compared to the structure of E106A-CAII, the sulfate sulphur has moved 0.4 Å (shifts of the oxygen atoms, 0.4 to 0.6 Å) toward the hydrophobic side. One of the non-liganded sulfate oxygen atoms is 3.0 Å from the amide N of Thr-199 and 3.3 Å from Cζ2 of Trp-209. The distances and angles of the zinc coordination sphere are given in Table IVF.

DISCUSSION

A model for the catalytic mechanism of carbonic anhydrase is shown schematically in Figure 12. According to the current hypothesis, the hydrogen-bond network involving Glu-106 and Thr-199 in the active site of CA serves to position a zinc-bound hydroxide ion in an optimal orientation for a nucleophilic attack on the CO_2 substrate.[5–8,11,24] We have shown that the disruption of this network by site-specific mutagenesis has drastic effects on the catalytic activity[11] as well as subtle, but distinct effects on the molecular structure.

The replacement of Thr-199 with Ala not only removes the hydrogen-bond between residue 199 and the zinc-bound H_2O/OH^- but also leads to a distortion of the tetrahedral zinc geometry. In addition, one may assume that the zinc-bound H_2O/OH^- has gained rotational freedom in the mutant. Thus, both the position and the orientation of the reactive hydroxide ion have changed, and this subtle structural

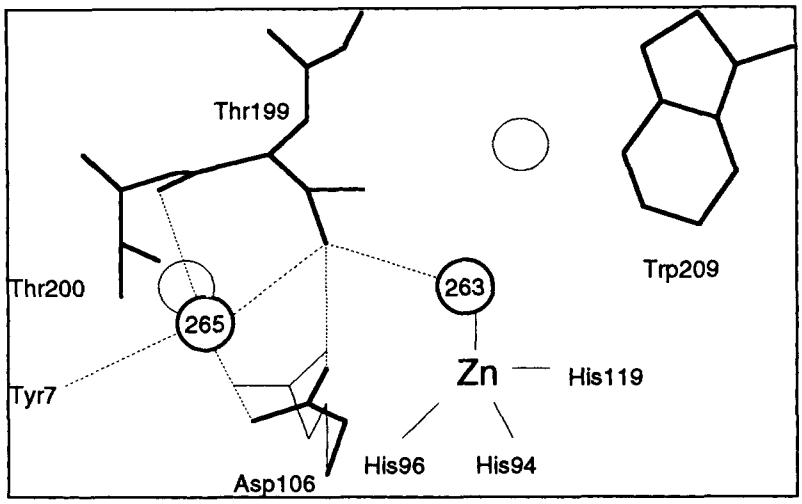

Fig. 11. Schematic diagram of the active site of E106D-CAII. The zinc-bound water molecule, Wat263, has a partial occupancy only, and a sulfate ion (not shown) was also shown to be bound to the zinc ion with a partial occupancy. Circles in thin lines indicate water positions in the native enzyme. The position of the side chain of Glu-106 in native CAII is shown by thin lines.

change is associated with a 100-fold decrease of the catalytic activity as expressed in k_{cat} as well as in k_{cat}/K_m for CO_2 hydration.[11]

Despite the extra space caused by the mutation and the removal of the requirement of a hydrogen-bond donor at the "tetrahedral" position on the zinc ion, sulfate seems to be excluded from the active site although this ion is present at a high concentration in the crystallization medium. This is probably due to Glu-106 which has become accessible from the active site by the removal of the γ atoms of Thr-199. Assuming that Glu-106 is ionized,[25] we observe that its negative charge is close to the zinc ion but not close enough for direct coordination. Instead, the zinc-bound H_2O/OH^- has moved towards Glu-106 to form a (long) hydrogen bond with it. This interaction should affect the ionization behavior as well as the nucleophilicity of the zinc-bound H_2O/OH^- and, hence, the catalytic activity of the enzyme.

In the bicarbonate complex of the mutant with Ala-199, the zinc-bound water is not displaced. Instead, it has moved closer to Glu-106 and one bicarbonate oxygen has bound to the metal ion in a pentacoordinated arrangement. It seems likely that this bicarbonate oxygen is unprotonated and that the zinc-bound water molecule is unionized in the complex. The protonated bicarbonate oxygen is probably the one pointing into the hydrophobic cavity, since the third oxygen atom seems to act as an acceptor in hydrogen bonds with the zinc-bound water molecule as well as with the amide NH of Ala-199.

This bicarbonate binding mode is different from that observed for the catalytically competent mutant, T200H-CAII.[9] In this mutant, bicarbonate displaces the zinc-bound H_2O/OH^- and binds in a pseudo-bidentate manner with the protonated oxygen 2.2 Å from the zinc ion and hydrogen bonded to Thr-199, while one of the unprotonated oxygens is located 2.5 Å from the zinc ion. A third bicarbonate binding mode has been observed in the crystal structure of Co(II)-substituted CAII.[26] In this case, the metal-bound water remains and two bicarbonate oxygens are located at equal, but rather long (2.4 Å), distances from the metal ion. One of these oxygen atoms is probably protonated since it is hydrogen bonded to the hydroxyl oxygen of Thr-199.[26] One can envisage that the bicarbonate product of CO_2 hydration catalyzed by native CAII is first bound as in T200H-CAII, but is displaced from the metal ion by a water molecule via intermediates with structures similar to those observed for the bicarbonate complexes of Co(II)-substituted CAII and T199A-CAII.

Remarkably, a bidentate binding of bicarbonate with "normal" (about 2.0 Å) metal–oxygen distances has so far not been found experimentally. Presumably, the hydrogen-bonding requirements imposed by Thr-199 combined with the negative charge of Glu-106 as well as steric factors hinder bicarbonate from binding in this manner. Indeed, only one example of "normal" pentacoordination has yet been found in crystal structure studies of catalytically competent forms of CAII, namely the SCN^- complex with native enzyme, where the anion occupies the fifth coordination site without displacing the zinc-bound water molecule.[6] Thus, it seems as if the presence of Thr-199 leads to a strong preference for tetracoordination or pseudo-pentacoordination of the zinc ion in CA.

The tetrahedral coordination geometry of the zinc ion is maintained when Glu-106 is changed to Ala or Gln. Apparently, the steering effect of Thr-199 is not completely lost in these mutants. However, our results suggest that the directionality of the hydrogen-

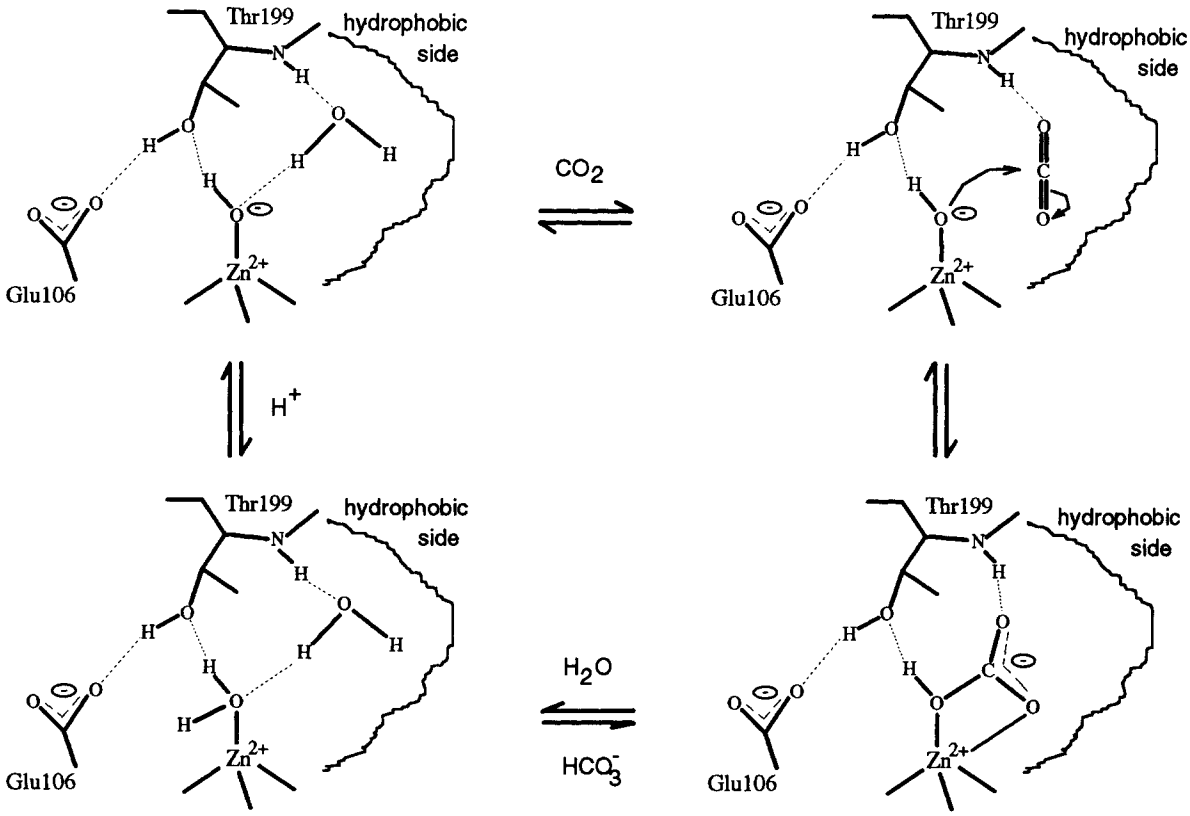

Fig. 12. Schematic diagram of the current hypothesis for the catalytic mechanism of carbonic anhydrase. The interconversion between CO_2 and HCO_3^- is emphasized, while the details of the reactions involved in the transfer of a proton from the zinc-bound water molecule to the reaction medium have been left out. The enzyme–bicarbonate complex is drawn as observed in the crystal structure of the mutant T200H-CAII.[9]

bonding interaction between Thr-199 and the "tetrahedral" zinc ligand depends on residue 106. This is particularly apparent in the mutant with Gln-106, where the hydrogen-bond connection between residue 106 and Thr-199 is maintained, although the amide NH_2 group of Gln-106 must donate a proton in the bond with the hydroxyl group of Thr-199, which interacts as a hydrogen-bond donor with the "tetrahedral" zinc ligand. This change of directionality seems to remove the preference for a protonated ligand atom at the "tetrahedral" position on the metal ion, while the loss of a negative charge in the mutants with Ala-106 or Gln-106 probably is important for removing the discrimination against the binding of doubly charged anions. These considerations may serve as explanations of the rather strong binding of sulfate in these mutants. However, a weakly bound sulfate ion was also observed in the mutant with Asp-106. This mutant has almost full catalytic activity.[11] The replacement of Glu-106 with Asp results only in rather small and subtle structural changes, but these apparently suffice to change the affinity for sulfate significantly. Native CAII is inhibited by sulfate below pH 7,[27] but at least part if not all of this inhibition can be interpreted as an ionic strength effect on the pK_a of the zinc-bound water.[28] In fact, zinc-bound sulfate has not been observed in X-ray studies of native CAII crystals equilibrated with high sulfate concentrations at pH values as low as 5.7.[7,29]

The kinetic properties of the mutants with Ala-106 and Gln-106 in sulfate-free media suggest that the rates of $CO_2 \rightarrow HCO_3^-$ interconversion in the active site, as reflected in the values of k_{cat}/K_m for CO_2 hydration, are only moderately affected by these alterations. The observed 1000-fold decrease of the maximal rate of CO_2 hydration, k_{cat}, caused by these mutations might be due to a decrease of the HCO_3^- dissociation rate and/or the rate of transfer of a proton from the active site to the reaction medium.[11] Although the crystal structures of these mutants without bound sulfate are not yet known, we venture the hypothesis that the position of a zinc-bound hydroxide ion is nearly the same as in native CAII due to the presence of Thr-199 and that it can have an appropriate orientation relative to the CO_2 substrate for a significant fraction of the time.

In summary, the results of our studies of CAII mutants suggest that the hydrogen-bond network involving Glu-106 and Thr-199 is of crucial impor-

tance for the catalytic function of the enzyme. These two residues seem to operate in conjunction to control the precise coordination geometry and binding selectivity of the metal ion. They seem to ensure a unique environment for a zinc-bound water molecule and an optimal orientation of a zinc-bound hydroxide ion for an efficient attack on carbon dioxide.

ACKNOWLEDGMENTS

We are grateful to Kjell Håkansson, Anders Svensson, and Jukka Vidgren for their help at various stages of this project. This work was financially supported by grants from the Swedish Natural Science Research Council (NFR) and the Swedish National Board for Industrial and Technical Development (NUTEK). The crystallographic equipment was financed by grants from the Swedish Council for Planning and Coordination of Research (FRN), the SE-bank and the Knut and Alice Wallenberg foundation.

REFERENCES

1. Silverman, D.N., Lindskog, S. The catalytic mechanism of carbonic anhydrase: Implications of a rate limiting protolysis of water. Acc. Chem. Res. 21:30–36, 1988.
2. Alexander, R.S., Nair, S.K., Christianson, D.W. Engineering the hydrophobic pocket of carbonic anhydrase II. Biochemistry 30:11064–11072, 1991.
3. Eriksson, A.E., Jones, T.A., Liljas, A. The refined structure of human carbonic anhydrase II at 2.0 Å resolution. Proteins 4:274–282, 1988.
4. Tashian, R.E. The carbonic anhydrases. Widening perspectives on their evolution, expression and function. BioEssays 10:186–192, 1989.
5. Merz, K.M. Insights into the function of the zinc hydroxide-Thr 199-Glu 106 hydrogen bonding network in carbonic anhydrases. J. Mol. Biol. 214:799–802, 1990.
6. Eriksson, A.E. Kylsten, P.M., Jones, T.A., Liljas, A. Crystallographic studies of inhibitor binding sites in human carbonic anhydrase II: A penta-coordinated binding of the SCN^- ion to the zinc at high pH. Proteins 4:283–293, 1988.
7. Håkansson, K., Carlsson, M., Svensson, A.L., Liljas, A. The structure of native and apo carbonic anhydrase II and some of its anion complexes. J. Mol. Biol. 227:1192–1204, 1992.
8. Lindahl, M., Svensson, A.L., Liljas, A. Metal poison inhibition of carbonic anhydrase. Proteins 15:177–182, 1993.
9. Xue, Y., Vidgren, J., Svensson, A.L., Liljas, A., Jonsson, B.-H., Lindskog, S. Crystallographic analysis of Thr200 → His human carbonic anhydrase II and its complex with the substrate, HCO_3^-. Proteins 15:80–87, 1993.
10. Liang, J.-Y., Lipscomb, W.N. Hydration of carbon dioxide by carbonic anhydrase: Internal proton transfer of Zn^{2+}-bound HCO_3^-. Biochemistry 26:5293–5301, 1987.
11. Liang, Z., Xue, Y., Behravan, G., Jonsson, B.-H., Lindskog, S. Importance of the conserved active-site residues Tyr 7, Glu 106 and Thr 199 for the catalytic function of human carbonic anhydrase II. Eur. J. Biochem. 211:821–827, 1993.
12. Khalifah, R.G., Strader, D.J., Bryant, S.H., Gibson, S.M. Carbon-13 nuclear magnetic resonance probe of active-site ionizations in human carbonic anhydrase B. Biochemistry 16:2241–2247, 1977.
13. Xue, Y., Jonsson, B.-H. Unpublished results.
14. Howard, A.J., Gilliland, G.L., Finzel, B.C., Poulos, T.L., Ohlendorf, D.H., Salemme, F.R. The use of an imaging proportional counter in macromolecular crystallography. J. Appl. Crystallogr. 20:383–387, 1987.
15. Blum, M., Metcalf, P., Harrison, S.C. & Wiley, D.C. A system for collection and on-line integration of X-ray diffraction data from a multiwire area detector. J. Appl. Crystallogr. 20:235–242, 1987.
16. Kabsch, W. Evaluation of single crystal X-ray diffraction data from a position sensitive detector. J. Appl. Crystallogr. 21:916–924, 1988.
17. CCP4, 1979, The SERC (UK) collaborative computing project no. 4. A suite of programs for protein crystallography distributed from Daresbury Laboratory, Warrington, WA4 4AD, UK.
18. Jones, T.A. A graphics model building and refinement system for macromolecules. J. Appl. Crystallogr. 11:268–272, 1978.
19. Jones, T.A. FRODO: A graphics fitting program for macromolecules. In "Computational Crystallography." Sayre, D. (ed.). Oxford: Clarendon Press, 1982: 303–317.
20. Jones, T.A., Zou, J.-Y., Cowan, S.W., Kjeldgaard, M. Improved methods for building protein models in electron density maps and the location of errors in these models. Acta Crystallogr. A47:110–119, 1991.
21. Hendrickson, W.A. Stereochemically restrained refinement of macromolecular structures. Methods Enzymol. 115:252–270, 1985.
22. Finzel, B.C. Incorporation of fast Fourier transforms to speed restrained least-squares refinement of protein structures. J. Appl. Crystallogr. 20:53–55, 1987.
23. Luzatti, V. Traitement statistique des erreur dans la determination des structures cristalline. Acta Crystallogr. 5:802–810, 1952.
24. Merz, K.M. CO_2 binding to human carbonic anhydrase II. J. Am. Chem. Soc. 113:406–411, 1991.
25. Merz, K.M. Determination of pK_as of ionizable groups in proteins: The pK_a of Glu 7 and 35 in hen egg white lysozyme and Glu 106 in human carbonic anhydrase II. J. Am. Chem. Soc. 113:3572–3575, 1991.
26. Håkansson, K., Wehnert, A. The structure of cobalt carbonic anhydrase complexed with bicarbonate. J. Mol. Biol. 228:1212–1218, 1992.
27. Simonsson, I., Lindskog, S. The interaction of sulfate with carbonic anhydrase. Eur. J. Biochem. 123:29–36, 1982.
28. Pocker, Y., Miao, C.H. Molecular basis of ionic strength effects: Interaction of enzyme and sulfate ion in CO_2 hydration and HCO_3^- dehydration reactions catalyzed by carbonic anhydrase II. Biochemistry 26:8481–8486, 1987.
29. Nair, S.K., Christianson, D.W. Unexpected pH-dependent conformation of His-64, the proton shuttle of carbonic anhydrase II. J. Am. Chem. Soc. 113:9455–9458, 1991.